ORIGINAL RESEARCH PAPER

Occurrence of arc interaction in tandem pulsed gas metal arc welding

T. Ueyama*, T. Ohnawa, M. Tanaka and K. Nakata

In the tandem pulsed gas metal arc welding, the occurrence of arc interruption by the electromagnetic interaction between the two adjacent arcs becomes a problem. In order to clarify this problem, effects of interwire distance and Ar–CO_2 gas mixture ratio on an abnormal arc voltage and arc interruption are investigated. The abnormal arc voltage and the arc interruption frequently occur with pulse peak currents which are supplied alternately to two wires. In addition, both phenomena occur in trailing arc which is located on molten pool at base current duration remarkably. There is most number of abnormal arc voltage and arc interruption times in trailing when the interwire distance is 10 mm, because a deflected length of trailing arc by the electromagnetic interaction becomes the longest. Moreover, the CO_2 mixture ratio in shielded gas affects the occurrence of abnormal arc voltage and arc interruption. The abnormal arc voltage and arc interruption do not occur when CO_2 gas mixture ratio is equal to or less than 5%. However, number of abnormal arc voltage and arc interruption times increase rapidly with increasing CO_2 gas mixture ratio when CO_2 gas mixture ratio is over 10%.

Keywords: Tandem, GMA welding, Pulse current, Arc stability, Arc interaction, Interwire distance, Shielded gas

Introduction

In tandem pulsed gas metal arc welding (TPGMAW), a couple of arcs closely generate, and these arcs can interact with each other affected by the magnetic fields generated around the individual arcs.[1,2] When the two wires are connected to the same polarity, the two arcs can be attracted each other between the two wires. Consequently, the states of the arcs become unstable, causing arc interruptions, irregular metal transfers and the resultant much spatter. In addition, the arc interaction can cause the fluctuation of arc voltage, and thereby the arc length control by the welding power sources becomes unstable, causing deteriorated weld bead formation. Therefore, in order to obtain sound welds with the TPGMAW, the arc interaction must be prevented to make the arc length control stable and thereby obtain smooth metal transfer.

When pulsed arc is employed in TPGMAW, it is reportedly proper to supply pulse peak currents and base currents at alternative timing for the two wires (reverse phase).[2–8]

The authors studied the effects of the configuration of the two wires on the formation of weld bead in high speed welding of steel sheets, and showed that high speed welding ability could be maximised where the interwire distance was 9 to 12 mm with a shielded gas of 80Ar–20CO_2 mixture.[9] In this case, welding was performed without the pulse timing control for the welding currents supplied to the two wires. Consequently, momentary arc interruptions and long term arc interruptions were often observed for the leading and trailing arcs. By contrast, in the TPGMAW of aluminium alloys using pure argon gas shielding, it was confirmed that arc interruption seldom occurred regardless of the presence or absence of the pulse timing control for the welding currents supplied to the two wires.[10] From these facts, it can be considered that not only the presence or absence of the pulse timing control for the welding currents supplied to the two wires, but also the interwire distance of the adjacent wires and shielded gas composition affect the occurrence of arc interruption.

The authors have investigated the factors affecting the arc interaction between the leading and trailing arcs and the resultant arc interruption in TPGMAW and clarified in this report the effects of interwire distance and shielded gas composition on such problems.

Experimental

Experimental materials

The base metal of mild steel sheet 3·2 mm thick, 65 mm wide and 450 mm long was used; the welding solid wire had a diameter of 1·2 mm. To investigate the effect of shielded gas composition on arc interruption, premixed Ar–CO_2 gases containing 2, 5, 10, 15, 20, 25%CO_2 respectively in the balancing Ar gas were used at a flowrate of 50 L min^{-1}.

Experimental procedure

Figure 1 shows the experimental setup of TPGMAW system used for this study. This experimental system

Department of Welding Research, DAIHEN Corporation, 5-1 Minami, Senrioka, Settsu, Osaka, Japan

*Corresponding author, email ueyama@daihen.co.jp

Published by Maney on behalf of the Institute
Received 28 December 2006; accepted 29 December 2006
DOI 10.1179/174329307X173715

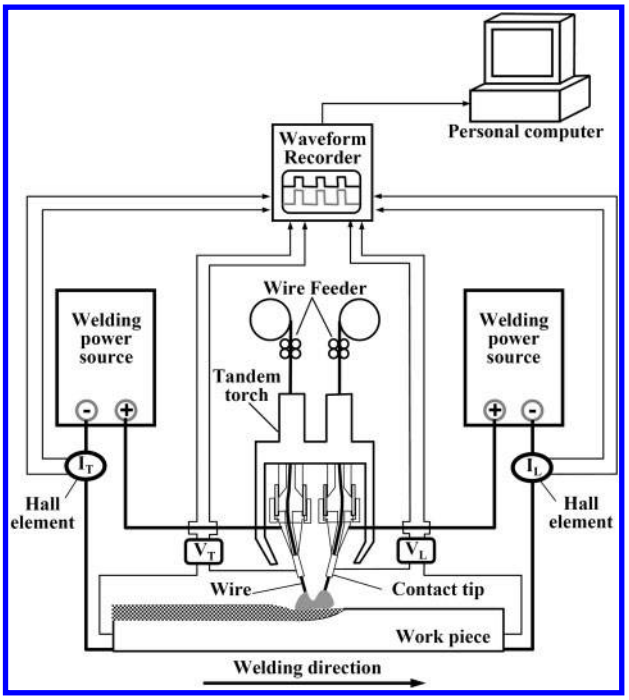

1 Experimental apparatus arrangements for analysing current and voltage wave form of TPGMAW

used two digital inverter controlled pulsed GMA welding power sources rated at a output of 500 A respectively, each of which was connected to the individual contact tips installed in a custom made experimental torch[9] that enabled to set the interwire distance in several steps from 5 to 20 mm. In this experiment, the pulse timing control between the two power sources was not employed.

A waveform recorder (MEMORY HiCORDER 8841 made by HIOKI) was used for recording the waveforms of welding current and arc voltage. The welding currents for leading and trailing wires were measured with clamp meters, and the arc voltages were measured between the individual contact tips and the base metal. The waveforms of welding current and arc voltage were recorded by the waveform recorder for 7 s out of 9 s of one bead welding time, cutting out one second for each of the start and end periods of welding. The recorded waveform data were input in a personal computer to analyse statistically the number of abnormal arc voltage increases and arc interruptions that were caused by the arc interaction.

The threshold value for counting abnormal increases in arc voltage (abnormal arc voltage) was set at 50 V. This was because the arc voltage was maintained at ~40 V during the pulse peak current period in the stable welding condition, and the rated output of the power sources was 500 A/50 V. Thus the momentary maximum voltage that could be controlled was 50 V, and therefore a voltage increase exceeding 50 V could not be considered to be related with the power source control.

Table 1 shows the pulse current waveform parameters and welding conditions for TPGMAW employed in this experiment. The tip to base metal distance was set at 20 mm, and the pulse parameters of currents supplied to the leading and trailing wires and the wire feed speeds were set at the common values. The arc voltage was set at the proper value to obtain a particular arc length

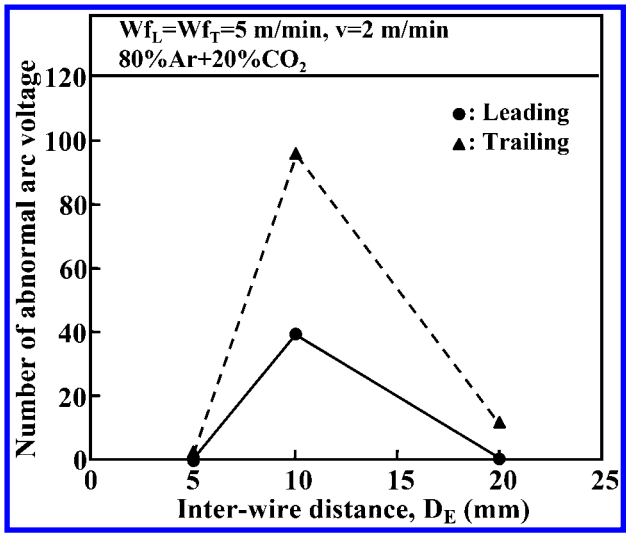

2 Effect of D_E on abnormal arc voltage

where short circuiting occurred at several times per second during the pulsed spray arc transfer. Bead on plate welding in the flat position was carried out for a welding length of 300 mm (welding time: 9 s) at a welding speed of 2 m min^{-1}.

A high speed digital video camera was used to investigate the arc interaction. The tandem welding torch was fixed, and the base metal was conveyed by a single axis X-table actuator that was set at the height where the welding arcs could reach the base metal, and the high speed video camera was positioned perpendicularly to the welding direction. In order to observe precisely, the behaviour of the arc plasma was recorded at 8000 frames s^{-1}, using no auxiliary lights such as Xenon back lights. During the high speed video recording the image frames were synchronised to the waveforms of welding current and arc voltage.

Effects of interwire distance on arc interaction

Figure 2 shows the effect of interwire distance D_E on the number of abnormal arc voltages for the leading and trailing arcs. When D_E was 5 mm, the number of abnormal arc voltage was 0 for both the leading and trailing arcs. When D_E was 10 mm, it sharply increased to 38 times for the leading arc and 89 times for the trailing arc. However, when D_E was 20 mm, it decreased to 0 for the leading arc and 11 times for the trailing arc.

Figure 3 shows the effect of interwire distance on the number of arc interruptions. There was no arc interruption in both the leading and trailing arcs when the interwire distance D_E was 5 mm. When the interwire distance D_E was 10 mm, the number of arc interruptions increased to 5 times for the leading arc and 23 times for the trailing arc, but when the interwire distance D_E was 20 mm, it decreased to be none for the leading arc and 3

Table 1 Experimental conditions

Pulse peak current I_P	450 A
Pulse peak duration T_P	1·5 ms
Base current I_B	45 A
Wire feed rate W_f	5 m min^{-1}
Welding speed v	2 m min^{-1}
Interwire distance D_E	5, 10, 20 mm

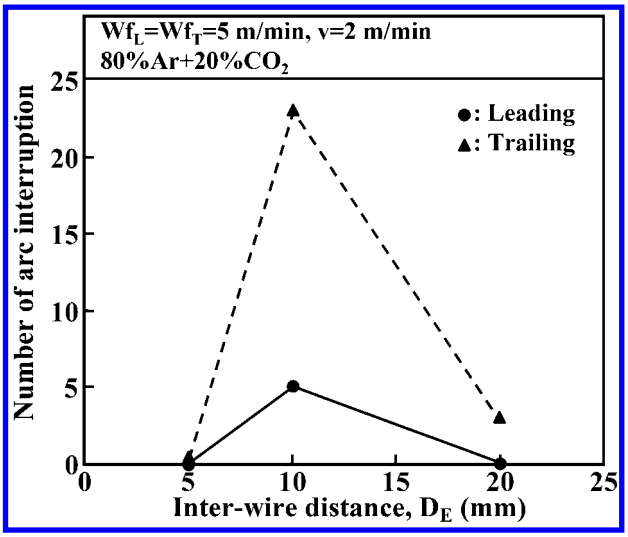

3 Effect of D_E on arc interruption

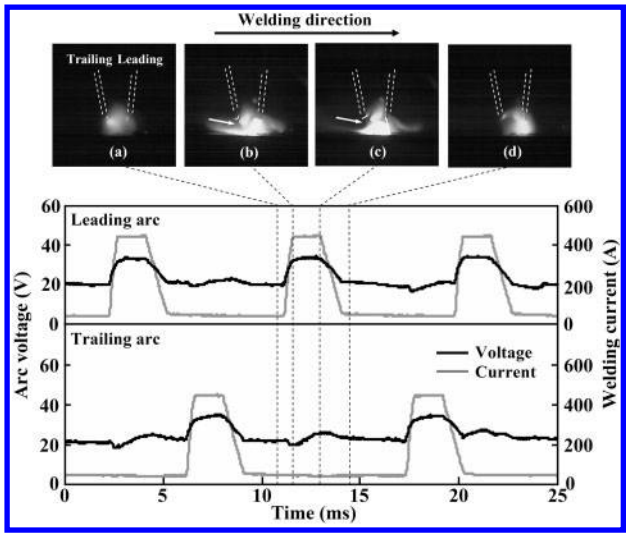

4 Arc phenomenon in TPGMAW at D_E=5 mm

times for the trailing arc, which coincided with the tendency of the number of abnormal arc voltage shown in Fig. 2.

Figure 4 shows the arc phenomenon observed in the reverse phase period with 5 mm D_E. As shown in the figure, the trailing arc was touching the leading wire and the leading arc was touching the trailing wire alternatively, because the D_E was short. Therefore, the current path for each of the wires was secured all the time even when the one was at base current and the other at pulse peak current.

In addition, as indicated with arrows in the frames (b) and (c), the trailing arc in the base current period was observed to be attracted to the leading arc where pulse peak current was supplied. Since the cathode spots did not move away from the weld pool underneath the trailing wire, neither abnormal arc voltage increased nor arc interruption was thought to occur.

Figure 5 shows abnormal increases in the trailing arc voltage in the reverse phase period with 10 mm D_E. In this period when base currents were supplied to both the leading and trailing arcs, as shown in the frame (a),

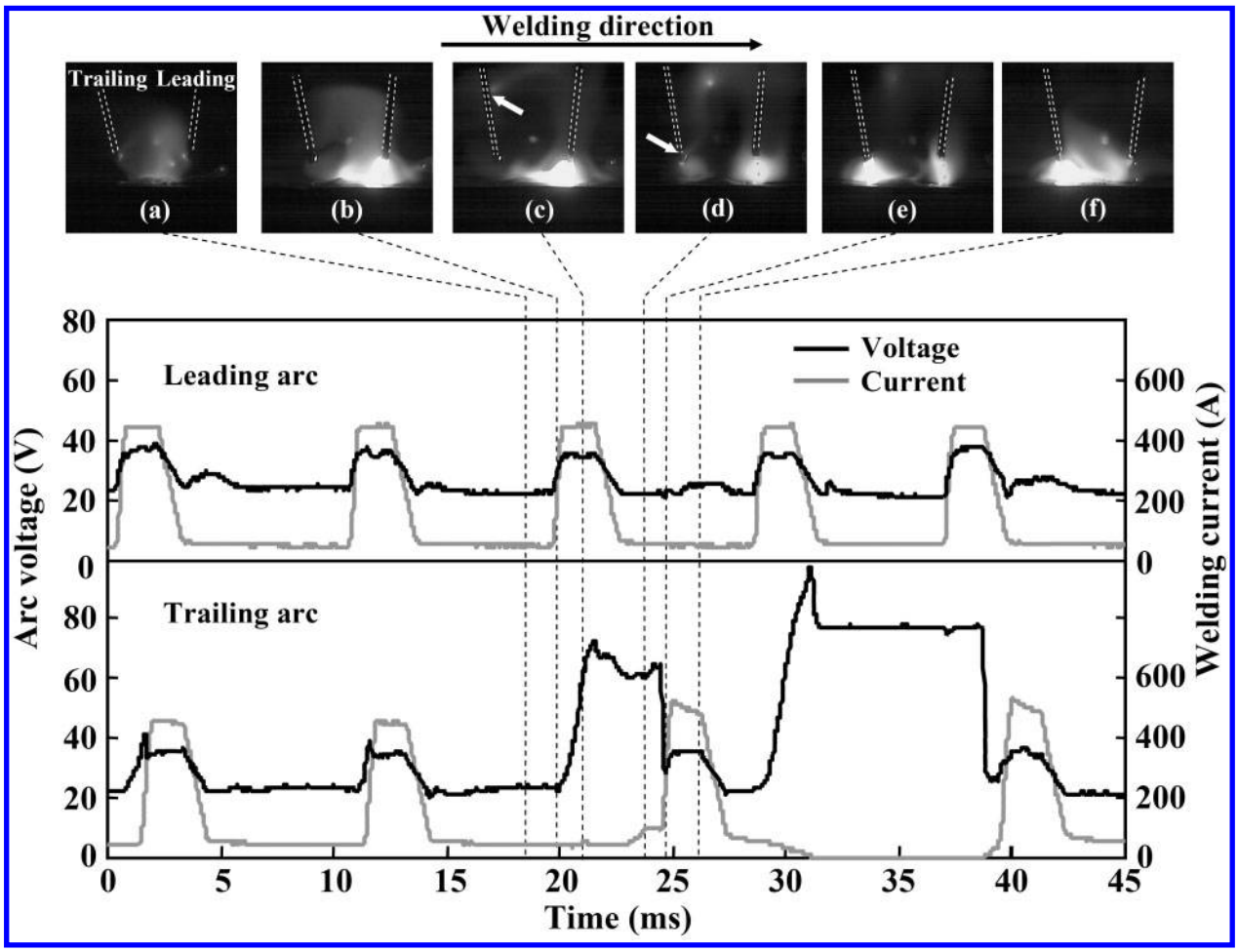

5 Abnormal arc voltage occurring on trailing arc at D_E=10 mm

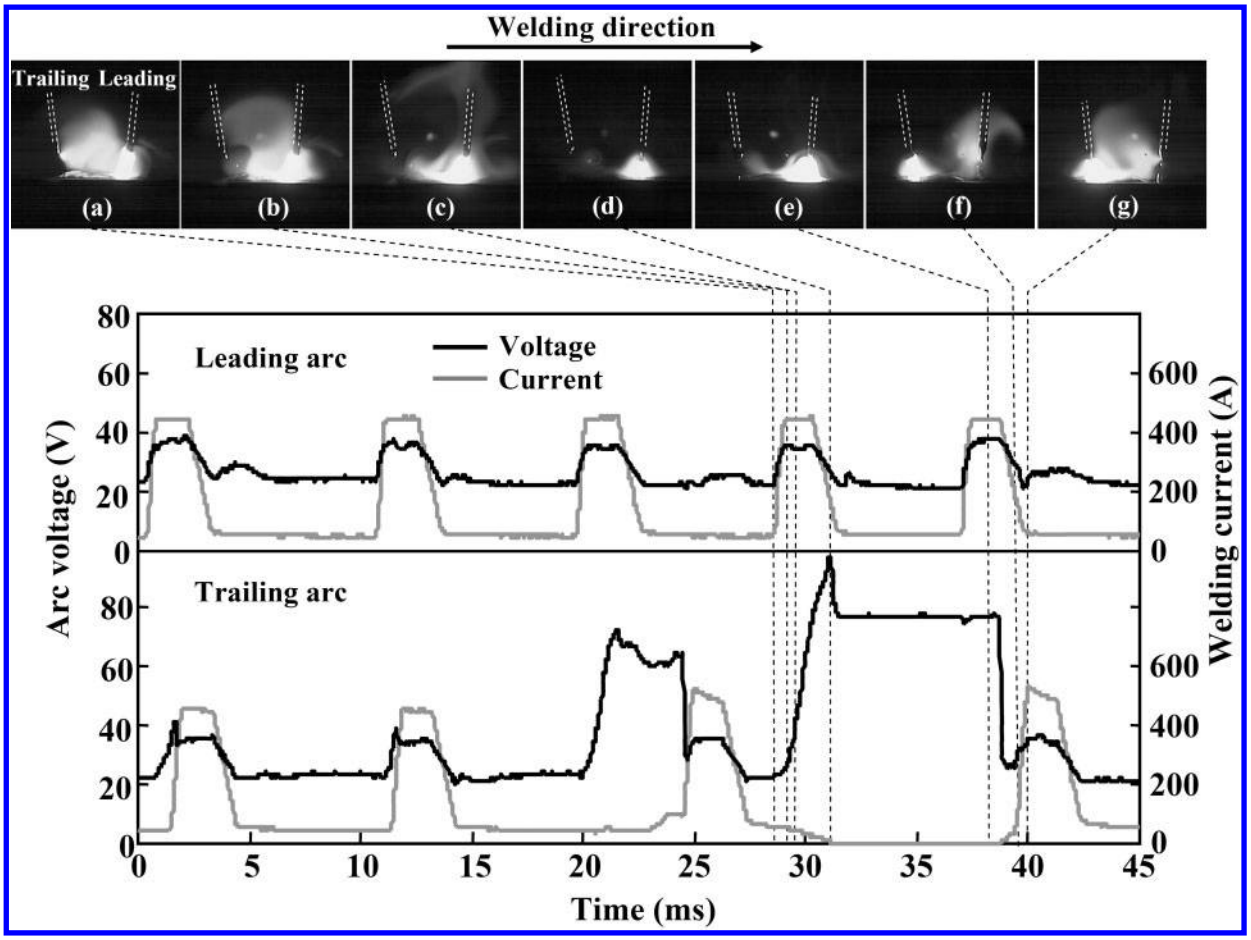

6 Arc interruption and reignition on trailing arc at D_E=10 mm

dimly gleaming arc plasmas were observed to be attracted between the individual wires. When the pulse peak current began to be supplied to the leading wire, as shown in the frame (b), the trailing arc root moved rapidly from the vicinity of the weld pool underneath the trailing wire to the vicinity of the weld pool underneath the leading wire, and at the same time, the arc plasma of the trailing arc was curved and elongated upwards by the electromagnetic force. While the pulse peak current was being supplied to the leading wire, the trailing arc plasma was curved and elongated further upwards as indicated with an arrow in the frame (c). At this time, the anode spot moved upwards along the wire as if it were dragged; consequently, the arc voltage increased. When the pulse peak current began to be supplied to the trailing wire, as indicated with an arrow in the frame (d), the anode spot ran down toward the tip of the wire caused by the increased stiffness of the arc.[10] At this moment, part of a cluster of cathode spots presumably maintained the arc root apart from the area underneath the trailing wire; and the curved arc plasma elongated still longer to cause a momentary increase in the arc voltage. Consequently, the output load of the welding power source increased, and the current increase to the pulse peak current was stopped for a certain time. However, just after that, the cathode spot presumably moved to the vicinity of the weld pool underneath the trailing arc on the surface of the base metal, as shown in the frames (e) and (f); as a result, the arc voltage decreased rapidly, the pulse peak current rose up again to 500 A, and the trailing arc plasma which had been deflected by the leading arc recovered to be a stable pulsed arc. At this time, even though the pulse peak current was being supplied to the trailing arc, the leading arc together with the arc root were not deflected towards the trailing arc, remaining on the surface of the base metal around the weld pool underneath the leading wire. Hence, abnormal increase in arc voltage did not occur in the leading arc in the base current period, even though the trailing arc current increased to the pulse peak value.

Figure 6 shows an arc interruption occurred after the arc phenomenon shown in Fig. 5. In the frames from (a) to (c), the arc phenomenon similar to that shown in Fig. 5 occurred. After a certain period of such situation, as shown in the frame (d), the arc voltage exceeded the no-load voltage (80 V) of the trailing side welding power source, and thereby the arc was extinguished. At this time, the output voltage increased up to $\sim$90 V after it exceeded the no-load voltage. This was because the voltage inducted by the inductance of the reactor of the power source was added to the output voltage. After the arc was extinguished, as shown in the frame (e), the leading arc expanded due to the pulse peak current of the next cycle and touched the trailing wire, and thereby the current path was presumably secured between the trailing wire and the base metal to ignite the arc again as shown in the frames (f) and (g).

When D_E was 10 mm, most of the arc interruptions that were occurred for either the leading or trailing arc were reignited induced by the arc plasma that was expanded due to the pulse peak current of the next cycle supplied to the other arc in which no arc interruption

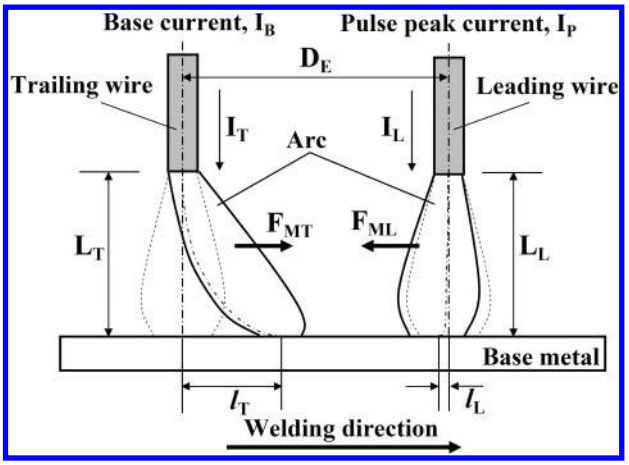

7 Schematic illustration of electromagnetic force acted on parallel two arcs

occurred. Therefore, when arc interruptions occurred, many of them lasted just for 10 ms or shorter.

Discussion of arc interaction

The frequencies of abnormal arc voltage and arc interruption for the leading and trailing arcs were confirmed to be the highest when the pulse currents supplied to the leading and trailing wires were in the reverse phase condition and the D_E was 10 mm. For discussing this reason, the authors make a simplified model and calculate the deflected lengths of two arcs which are attracted by mutual induced magnetic forces of each arc current.

Figure 7 shows a schematic illustration of the tandem arcs where the leading wire carries pulse peak currents and the trailing wire carries base currents in the reverse phase condition. In this case the leading and trailing arcs are mutually deflected inwards by the electromagnetic forces. The deflected lengths for the leading arc and for the trailing arc are l_L and l_T respectively.

The magnetic flux density around the trailing wire inducted by the leading arc, B_T, is

$$B_T = \frac{\mu_0 I_L}{2\pi D_E} \tag{1}$$

where D_E is the interwire distance, I_L is the leading arc current, and μ_0 is the permeability of free space. The electromagnetic force, namely, the Lorentz force F_{MT} induced by the magnetic flux density B_T with the trailing arc current is

$$F_{MT} = j_T \times B_T \tag{2}$$

where j_T is the current density of the trailing arc defined by $j_T = I_T/\pi r_T^2$, where I_t is the trailing arc current and r_T is the radius of the trailing arc column. Both arcs are assumed to be a magnetohydrodynamic fluid that flows from the anode (wire) to the cathode (base metal) respectively, and also both magnetohydrodynamic fluids are assumed to act on each Lorentz force F_{MT} and F_{ML}, like the gravity as shown in Fig. 7. Therefore, the deflected length, for example, for the trailing arc l_T is simply represented by a momentum equation

$$\rho_T \frac{d}{dt}\left(\frac{dl_T}{dt}\right) = F_{MT} \tag{3}$$

where ρ_T is the density of magnetohydrodynamic fluid for the trailing arc, and t is the time. The differential equation (3) gives an answer

$$l_T = \frac{F_{MT}}{2\rho_T} t^2 \tag{4}$$

within the boundary conditions; $dl_T/dt = 0$ and $l_T = 0$ at $t = 0$. When t is defined as the time required for the magnetohydrodynamic fluid to move from the anode (wire) to the cathode (base metal), t can be represented by

$$t = \frac{L_T}{u_T} \tag{5}$$

where L_T is the length of the trailing arc and u_T is the velocity of the magnetohydrodynamic fluid for the trailing arc, namely, the velocity of the plasma jet. Substitution of the equations (1), (2) and (5) into the equation (4) gives

$$l_T = \frac{\mu_0 j_T I_L}{4\rho_T \pi D_E}\left(\frac{L_T}{u_T}\right)^2 \tag{6}$$

and then the deflected length for the trailing arc l_T is simply estimated by this equation. The arc pressure close to the tip of the trailing wire can be given by the following equation[11]

$$P_T = \frac{\mu_0}{4\pi}\frac{I_T^2}{\pi r_T^2} \tag{7}$$

Here it is assumed that this arc pressure is perfectly transformed into the dynamic fluid flow of the arc close to the base metal, and then the Bernoulli equation[11,12] safely gives a following equation

$$P_T = \frac{\rho_T u_T^2}{2} \tag{8}$$

Substitution of the equation (7) into (8) gives

$$u_T^2 = \frac{2P_T}{\rho_T} = \frac{\mu_0 I_T^2}{2\pi^2 r_T^2 \rho_T} \tag{9}$$

Since $j_T = I_T/\pi r_T^2$, the equation (9) becomes

$$u_T^2 = \frac{\mu_0 I_T j_T}{2\pi\rho_T} \tag{10}$$

and then substitution of the equation (10) into the equation (6) gives

$$l_T = \frac{\mu_0 j_T I_L L_T^2}{4\pi\rho_T D_E}\cdot\frac{2\pi\rho_T}{\mu_0 I_T j_T} = \frac{I_L L_T^2}{2I_T D_E} \tag{11}$$

Hence, l_T can be just calculated from the I_L, I_T D_E and L_T. In the same way, the deflected length for the leading arc l_L can be also calculated from the I_L, I_T, D_E, and L_L by using the following equation

$$l_L = \frac{I_T L_L^2}{2I_L D_E} \tag{12}$$

In the case where the leading arc is at the pulse peak current $I_L = 450$ A and the trailing arc is at the base current $I_T = 45$ A in the reverse phase condition and the arc lengths L_L and L_T are 5 mm, the relationship between the D_E and the deflected lengths for the leading and trailing arcs can be calculated by the equations (11) and (12), and the result is shown in Fig. 8.

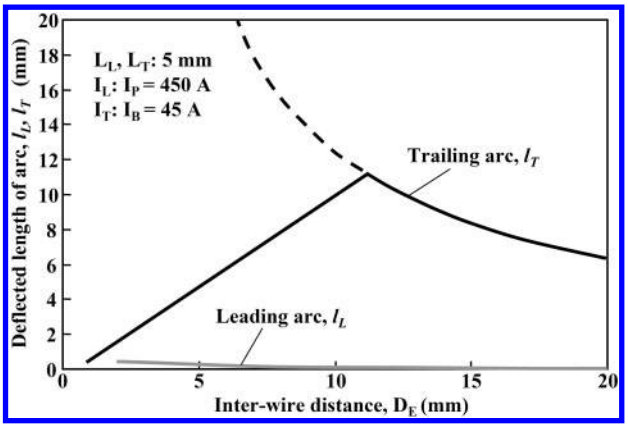

8 Relationship between D_E and deflected length of arc

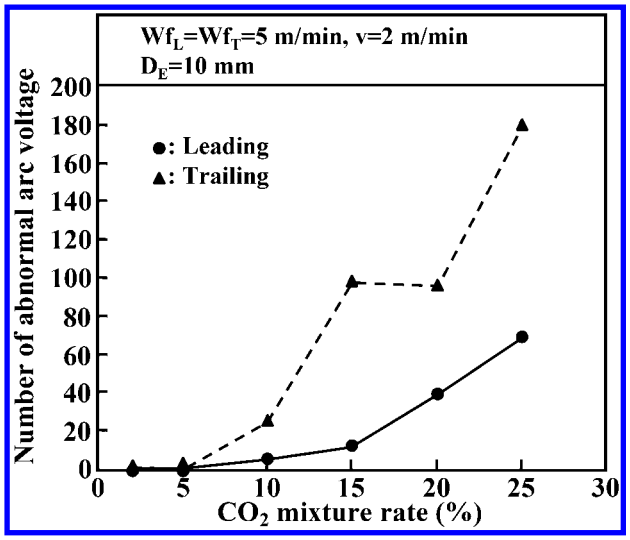

9 Effect of CO_2 mixture ratio on abnormal arc voltage

The deflected length for the trailing arc l_T becomes a maximum of 10·88 mm at 11 mm D_E, and this deflected length decreases with increasing D_E. When D_E is 11 mm or smaller, the deflected length increases with decreasing D_E, just in the calculation as shown by a dotted line. However, within the practical situation of the trailing arc, the trailing arc does not deflect exceeding the position of the opposite leading arc, namely, the trailing arc should not deflect further than the position where the trailing arc meets the arc root of the leading arc. From this assumption, the deflected length for the trailing arc can be estimated by subtracting the deflected length for the leading arc l_L from D_E, and then the deflected length decreases with decreasing D_E, where D_E is 11 mm or smaller, as shown by a solid line in Fig. 8. The deflected length for the leading arc l_L increases with decreasing D_E, but it is very small.

The above model can be calculated under the assumption that the arc root can easily move due to the Lorentz force induced by the arc current with the magnetic flux. Since the mild steel sheet used in this experiment has a thin oxide film on its surface, and then it is safely assumed that the cathode spot which forms the arc root moves freely. In fact, the calculations in Fig. 8 are in good agreement with the experimental relationship between D_E and the number of abnormal arc voltage or arc interruption for the trailing arc, as shown in Figs. 2 and 3 respectively. Numbers of the abnormal arc voltage and arc interruption became the highest at 10 mm in D_E where the deflected length for the trailing arc l_T becomes about the greatest in Fig. 8.

In the case where the leading arc is at base current and the trailing arc at pulse peak current, the relationship between D_E and the deflected length for the leading arc l_L becomes similar to that in Fig. 8 (although l_T and l_L must be replaced by each other). Although the frequencies of abnormal arc voltage and arc interruption in the case where the leading arc was at base current were clearly lower than in the case where the trailing arc was at base current, the tendency of relationship between D_E and numbers of abnormal arc voltage and arc interruption for the leading arc as shown in Figs. 2 and 3 respectively, was also in good agreement with the calculated relationship between D_E and the deflected length for the leading arc l_L.

Hence, the reason why abnormal arc voltage increase and arc interruption occur most frequently at 10 mm in D_E under the conditions of pulse currents supplied to the leading or trailing wires in the reverse phase can be discussed in the following way. The leading or trailing arc in the base current period is easily deflected at the greatest degree by the Lorentz force, the deflected arc plasma tends to be curved upwards in a complicated shape by the electromagnetic force and buoyant force, and thereby the length of arc discharge is apt to be longer. By contrast, when D_E is 20 mm, the deflection of the leading or trailing arc is less and then the arc discharge length tends to be hard to become longer, and as a result the frequencies of abnormal arc voltage decrease and arc interruption are assumed to be lower. When D_E is 5 mm, the Lorentz force which causes the arc deflection becomes bigger, but the arc deflection becomes less because the two arcs closely generate, thereby preventing the arc discharge length from becoming longer, securing the current path that shares the common arc root. Therefore, it can be considered that abnormal increase in arc voltage rarely occurs in this case.

Effect of shielded gas on arc interaction

Figure 9 shows the number of abnormal arc voltage as a function of CO_2 percentage in Ar–CO_2 mixture shielded gas when D_E was 10 mm. With 5% or lower CO_2, abnormal increase in arc voltage did not occur in the leading and trailing arcs. With 10% or higher CO_2, abnormal increase in arc voltage occurred 5 times in the leading arc and 24 times in the trailing arc; i.e. the number of abnormal arc voltage increases sharply increased for both the leading and trailing arcs with increasing CO_2 percentage. With a maximum of 25%CO_2, the number of abnormal increase in arc voltage was counted 68 times for the leading arc and 117 times for the trailing arc. Figure 10 shows the effect of CO_2 percentage in Ar–CO_2 mixture on the number of arc interruptions. The number of arc interruptions also increased with increasing CO_2 percentage for the leading and trailing arcs, and the increasing tendency is similar to that in Fig. 9, reaching two times or higher number of arc interruptions with 25%CO_2 than with 20%CO_2.

Figure 11 shows a comparison of the arc phenomena observed in this experiment in the reverse phase condition with 2 and 25%CO_2 respectively. With 2%CO_2, the arc plasma that generated at the leading

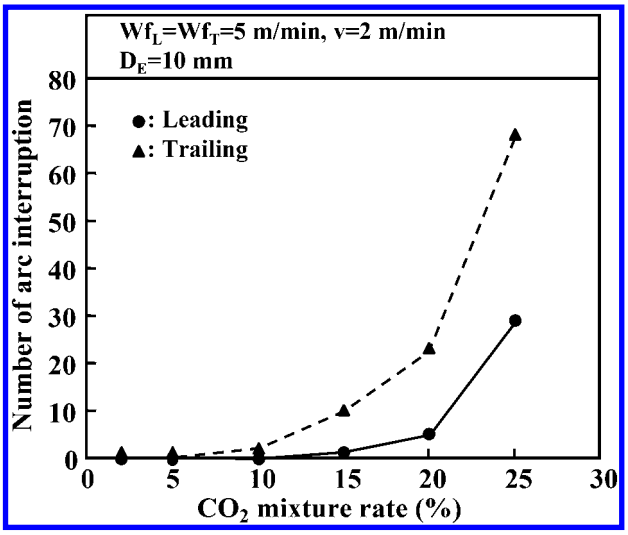

10 Effect of CO_2 mixture ratio on arc interruption

wire expanded widely so that it touched the trailing wire. Consequently the current path for the trailing arc can be assumed to have been secured with the leading arc plasma, and thereby no abnormal increase in arc voltage was observed even though the trailing arc was attracted by the leading arc. With 25%CO_2, the arc plasma generated at the leading wire was not expanded, and the arc was observed to be constricted due to the cooling effect caused by the dissociation of CO_2 gas. Then the trailing arc was attracted due to the effect of pulse peak currents supplied to the leading arc, yet the leading arc did not touch the trailing arc unlike with 2%CO_2. As a result, the base voltage of the trailing arc can be assumed to have increased up to an abnormally high level accompanied by the high arc voltage of the elongated trailing arc caused by the attraction force, in conjunction with the effect of high potential gradient[13] provided by high CO_2 percentage.

Conclusions

1. Abnormal arc voltage and the resultant arc interruption occurred in the reverse phase condition where one of tandem arcs was in the pulse peak current period and the other was in the base current period. The frequency of occurrence was higher in the reverse phase condition where the trailing arc was in the base current period.

2. The abnormal arc voltage and arc interruption occurred most frequently with 10 mm D_E, none of them occurred with 5 mm D_E, and they occurred less frequently with 20 mm D_E than with 10 mm D_E. This result coincided well with the calculation of the deflected length of the trailing arc root that was caused by

11 Comparison of arc phenomena between *a* 98Ar–2CO_2 and *b* 75Ar–25CO_2

the mutual attraction force induced between the two wires. That is, with the pulse waveform parameters set in this experiment for currents supplied to the two wires, the deflected length of the trailing arc root became a maximum with 11 mm D_E in the reverse phase condition.

3. The CO_2 percentage in an Ar–CO_2 mixture has a significant effect on abnormal arc voltage and arc interruption. That is, no abnormal arc voltage and arc interruption occurred with 5% or lower CO_2, but they increased sharply with 10% or higher CO_2.

References

1. D. Savu: 'Electromagnetic interactions in two wires MIG/MAG welding', IIW Doc. 212-944-99, IIW, 1999.
2. B. Yudodibroto, M. Hermans and I. Richardson: 'Process stability analysis during tandem wire arc welding', IIW Doc. XII-1876-06, 52–64, IIW, 2006.
3. U. Dilthey, U. Reisgen, H. Bachem and J. Gollnick: 'Two-wire process for higher deposition rate and higher welding speed', IIW Doc. XII-1549-98, 129–145, IIW, 1998.
4. S. Goecke, J. Hedegard and M. Lundin: *Svetsaren*, 2001, **56**, (2), 24–28.
5. D. Rehfeldt and T. Polte: 'Investigation on metal transfer in pulsed tandem MAG welding', IIW Doc. 212-967-00, IIW, 2000.
6. T. Morehead: *Weld. J.*, 2003, **82**, (6), 40–43.
7. J. Andersson, E. Tolf and J. Hedegard: 'The fundamental stability mechanism in tandem-MIG/MAG welding, and how to perform implementation', IIW Doc. XII-1895-06, 65–75, IIW, 2006.
8. B. Yudodibroto, M. Hermans and I. Richardson: 'The influence of pulse synchronization on the process stability during tandem wire arc welding', IIW Doc. XII-1910-06, 77–85, IIW, 2006.
9. T. Ueyama, T. Ohnawa, M. Tanaka and K. Nakata: *Sci. Technol. Weld. Join.*, 2005, **10**, (6), 750–759.
10. T. Ohnawa, T. Ueyama and T. Uezono: 'Tandem pulsed GMA welding method-comparison of the pulse timing control methods for mild steel and aluminum', Technical Commission on Welding Arc Physics of Japan Welding Society, 03-1216, Japan, 2003.
11. T. Ohji: 'Fundamentals of welding and jointing processes', 123–125; 1996, Sanpo Publications Inc, Tokyo.
12. J. F. Lancaster: 'The physics of welding', 80–81; 1984, Oxford, Pergamon Press.
13. K. Ando and M. Hasegawa: 'Phenomena of welding arc', Expanded edn, 106–107; 1967, Tokyo, Sanpo Publications Inc.